# Electromagnetic Forming of AZ31B Magnesium Alloy Sheet: Experimental Work and Numerical Simulation[*]

## I. Ulacia[1], J. Imbert[2], C.P. Salisbury[2], A. Arroyo[3], I. Hurtado[1], M.J. Worswick[2]

[1] Department of Manufacturing, Mondragon Goi Eskola Politeknikoa, University of Mondragon, Spain
[2] Department of Mechanical and Mechatronics Eng., University of Waterloo, Canada
[3] Automotive unit, Labein-Tecnalia Research Centre, Spain

## Abstract

*In the first stage of this work, polycrystalline specimens of AZ31B magnesium alloy have been characterized by uniaxial tensile tests at quasi-static and dynamic strain rates at room temperature. The influence of the strain rate is outlined and experimental results were fitted to the parameters of Johnson-Cook constitutive material model.*

*In the second stage of the present study, sheets of AZ31B magnesium alloy have been biaxially formed by electromagnetic forming using different coil and die configurations. Deformation values measured from electromagnetic formed parts are compared to the ones achieved with uniaxial tensile tests and also with the values obtained by conventional forming technologies.*

*Finally, numerical simulations have been carried out using an alternative method for computing the electromagnetic fields in the EMF process simulation, a combination of Finite Element Method (FEM) for conductor parts and Boundary Element Method (BEM) for the surrounding air (or more generally insulators) that is being implemented into commercial code LS-DYNA®.*

## Keywords

Electromagnetic sheet metal forming, Magnesium alloy, Formability, Numerical modelling

# 1 Introduction

Recently there is a clear tendency of reducing the weight of vehicles since lightening the final weight of the vehicle provides clear benefits in fuel economy [1]. For this reason, magnesium alloys are generating interest in the automotive and aeronautic industries, due to their low density in comparison to aluminium and steel alloys thereby reducing gross vehicular weight. In addition, the low density improves dent resistance and shell resistance behaviour by increasing thickness in structural sheet applications [2]. Currently, the use of magnesium alloys in a car is approximately 0.3% of the total weight of the vehicle; however, it is estimated that for the year 2020 the use of magnesium alloys in vehicles will increase to up to 12.2% of the total weight, mainly to the detriment of steel, iron and aluminium, as it is shown in Figure 1 [3].
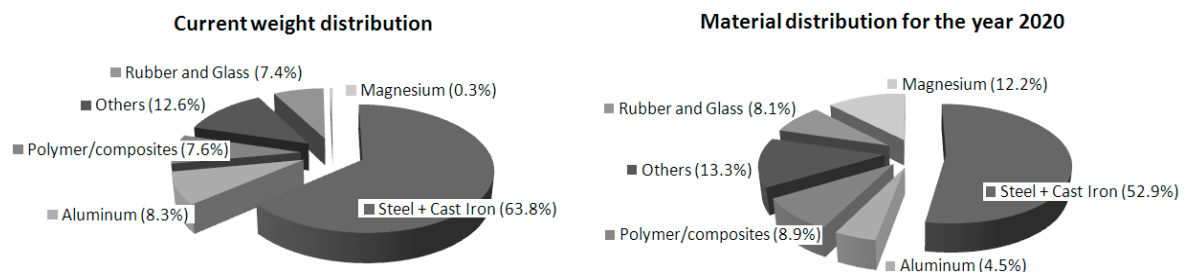


**Figure 1**: *Current and estimated weight distributions in a car [3]*

Some limitations appear when forming magnesium alloys due to the hexagonal close-packed (hcp) microstructure. It is for this reason that casting and forging technologies have traditionally been used to manufacture magnesium parts. It is a well known fact that the mechanical properties of parts obtained by deformation operations are higher than the properties obtained by casting. Consequently, if the formability of magnesium alloys could be improved, there would likely be a considerable increase in the use of this under-utilized material. Therefore, there is a clear need of new forming methods in order to overcome this limitation. One way of increasing the formability of magnesium alloys is to increase the forming temperature. This is due to the activation of prismatic $\{10\bar{1}0\} <11\bar{2}0>$ and pyramidal $\{10\bar{1}1\} <11\bar{2}0>$ slide planes which begins at temperatures around 200-225ºC leading to a considerable improvement of formability and reduction of the anisotropy [4,5]. Some studies [5,6] show interesting maximum limit drawing ratios (LDR) of 2.5 in a temperature range between 200-250ºC for AZ31 alloy.

Another way to increase the formability of magnesium alloys would be to employ high velocity forming technologies, such as electromagnetic forming. El-Magd *et al.* stated that for AZ80 magnesium alloy elongation increases under dynamic loading [7]. Very little work has been done in the field of high speed forming of magnesium alloys [8-11]; however, all the investigations agree that higher deformation values are achieved using electromagnetic pulses to deform magnesium alloys, concluding that EMF is a promising technology for processing magnesium parts, even at room temperature. The idea of combining inductive heating and pulsed magnetic forming for EMF at elevated temperatures was suggested by Uhlmann et al. [11]; unfortunately, they did not report any values of the achieved deformations.

Consequently, in the current work the suitability of electromagnetic forming to produce magnesium alloy parts is evaluated. In the first stage of the present work, AZ31B alloy is characterized under a wide range of strain rates in order to identify the effect of strain rate on the mechanical behaviour of this magnesium alloy. Furthermore, the experimental data is fitted to the Johnson-Cook constitutive model for the numerical simulation. After the material characterization, experimental work is shown. Different free forming configurations were employed in order to obtain a wide range of biaxial deformation state values. The final deformation values of the formed parts were measured by means of photogrammetric methods and a comparison with the limits obtained with conventional forming technologies is performed. In the final part of the current contribution, a coupled numerical model for the process simulation is presented and the results are compared with experimentally obtained parts.

## 2 Material Characterization

The material employed in this study was 1 mm thick sheet commercial available AZ31B-O magnesium alloy. Quasi-static and dynamic tensile tests were carried out in the strain rate range of $0.001 \text{ s}^{-1} < \dot{\varepsilon} < 1500 \text{ s}^{-1}$. The reader is referred to [12] for a more detailed description of the testing. In the current work, only the tests at room temperature are considered, neglecting the softening effect that occurs in the material due to the temperature rise from the adiabatic nature of the dynamic deformation.

### 2.1 Uniaxial Tensile Tests at Different Strain Rates

The material was tested in the laboratories of the University of Waterloo at three different strain rate ranges using three different testing techniques: i) quasi-static strain rate tests (0.001, 0.1 $\text{s}^{-1}$) were conducted in a conventional electromechanic drive INSTRON testing machine ii) for intermediate range (50, 80, 100 $\text{s}^{-1}$) an IMATEK Instrumented Falling Weight (IFWI) apparatus was used and iii) for high strain rate (500, 1000, 1500 $\text{s}^{-1}$) a tensile split Hopkinson bar (TSHB) was employed. The testing was done for both rolling and transversal direction. The experimental results for the different strain rate ranges are shown in Figure 2 (only typical curves are shown for clarity reasons). It can be clearly seen that for both directions increasing the strain rate also increases the flow stress.
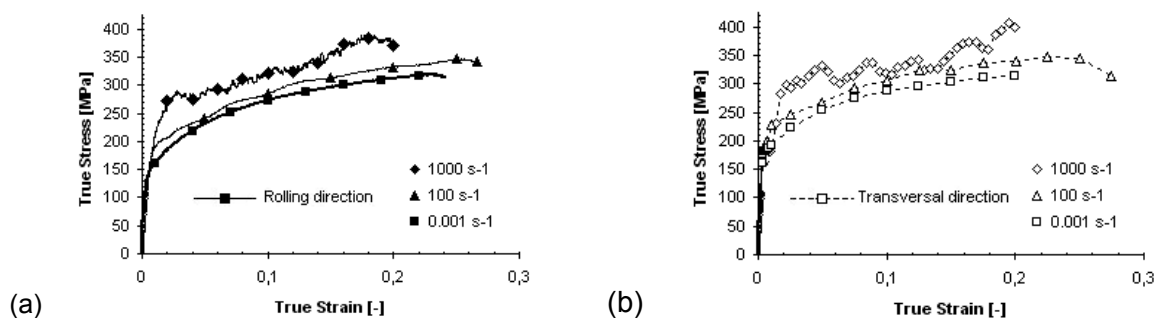


(a)          (b)

**Figure 2:** *Flow curves for AZ31B tests at different strain rates\**
*\*The reader is cautioned that in the high strain rate tests the loading to failure was not monotonic and therefore, the 1000 s-1 curve does not reach the real strain at fracture [12].*

The measured elongations at fracture are illustrated in Figure 3. It can be seen that initially, at quasi-static strain rate range, the ductility of the material decreases when increasing the strain rate. However at intermediate and high strain rate the elongation at fracture increases when the strain rate is also increased. The influence of the specimen direction in the ductility is less noticeable at high strain rates than at quasi-static range.
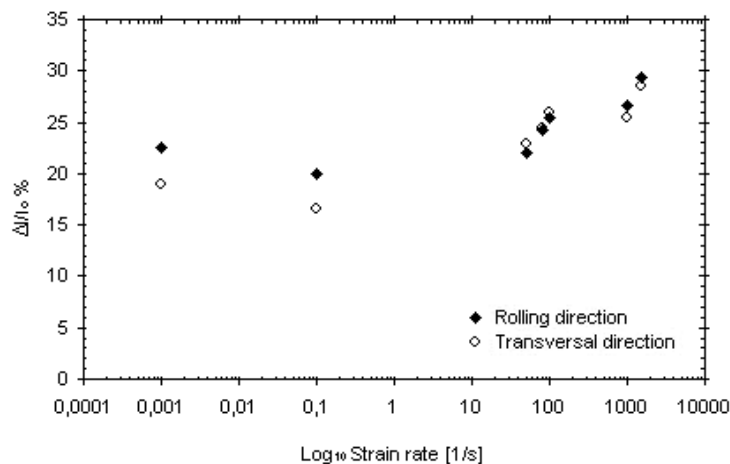


*Figure 3*: Elongation at fracture as a function of strain rate for AZ31B sheet

## 2.2   Constitutive Modelling

In order to model the constitutive response of the material for a wide range of strain rates, the flow stress can be determined as a function of effective plastic strain, strain rate and temperature using the constitutive equation of Johnson-Cook [13]:

$$\sigma = \left(A + B \cdot \varepsilon_{eps}^{n}\right) \cdot \left(1 + C \ln \frac{\dot{\varepsilon}}{\dot{\varepsilon}_0}\right) \cdot \left(1 - \left(\frac{T - T_{room}}{T_{melt} - T_{room}}\right)^{m}\right) \tag{1}$$

where $\varepsilon_{eps}$ is the effective plastic strain, $\dot{\varepsilon}$ is the strain rate, $\dot{\varepsilon}_0$ is the reference strain rate, $T$, $T_{room}$, $T_{melt}$ are respectively the current material temperature, room and melting temperature for the material. $A$, $B$, $C$, $n$ and $m$ are the five material constants. The final term in Equation 1 corresponding to thermal effects is not taken into account since temperature influence is neglected.

The constitutive parameters required by the Johnson-Cook constitutive model are fitted to the experimental results using a non linear regression technique. The estimated values of the parameters, for both rolling and transversal directions, are tabulated in Table 1 with their upper and lower bounds for a 95% confidence interval.

| Parameter | Estimate | 95% Confidence | |
| --- | --- | --- | --- |
| | | Lower Bound | Upper Bound |
| Rolling direction | | | |
| *A* (MPa) | 180.002 | 152.028 | 207.977 |
| *B* (MPa) | 344.548 | 309.940 | 379.156 |
| *n* | 0.554 | 0.329 | 0.613 |

| C | 0.012 | 0.010 | 0.013 |
|---|---|---|---|
| Transversal direction | | | |
| A (MPa) | 220.891 | 176.558 | 265.223 |
| B (MPa) | 205.583 | 182.989 | 228.178 |
| n | 0.370 | 0.144 | 0.596 |
| C | 0.011 | 0.010 | 0.013 |

**Table 1:** *Johnson-Cook parameters for AZ31B*

In Figure 4 constitutive model for AZ31B is shown. Good agreement is seen between experimental results and constitutive models. It is also observed that for the rolling direction the strain hardening rate is higher than for transversal direction.
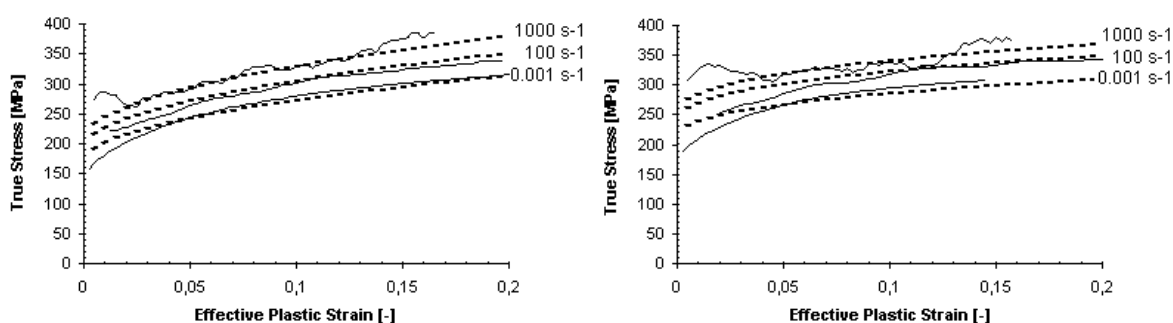


**Figure 4**: *Comparison of Johnson-Cook model predictions (dashed lines) with experimental results (solid lines) for rolling direction (left) and transversal direction (right)*

# 3 Experimental Work

## 3.1 Experimental Procedure

Different EMF experiments were carried out in the laboratories of Labein-Tecnalia with the aim of obtaining a wide range of deformations in the AZ31B magnesium sheets of 175 mm x 250 mm x 1 mm. Furthermore, electromagnetic forming experiments with an open die were performed in order to be recorded by means of a Photron FASTCAM-APX RS 250K high speed camera at a sampling rate of 37500 fps.

The multi-turn coil used for these experiments is made from copper as illustrated in Figure 5(a). Three different dies were employed in the experiments: i) a free forming square die with an 82 mm width and 160 mm in length, Figure 5(b); ii) a circular die with 80 mm in diameter, Figure 5(c); and iii) an elliptic die with the major and minor axis of 80 mm and 40 mm respectively, Figure 5(d). The die radius is 4 mm in all the cases. In some experiments with the circular and elliptic geometry, a driver of AA1050-0 aluminium alloy sheet of 1 mm thickness was used in order to reduce the discharged energy from a maximum value of 22 kJ to 7.5 kJ. In the case of square free forming die no driver was used due to the sheet-coil configuration (this point will be analysed with more detail in the numerical model section). A maximum energy of 4 kJ was discharged to form safe parts. A closing force of 60 kN was applied in all the cases by means of a hydraulic press. The discharged currents were measured at a sampling rate of 1.25 MHz by means of an oscilloscope connected to the Rogowsky coil of the EMF machine.
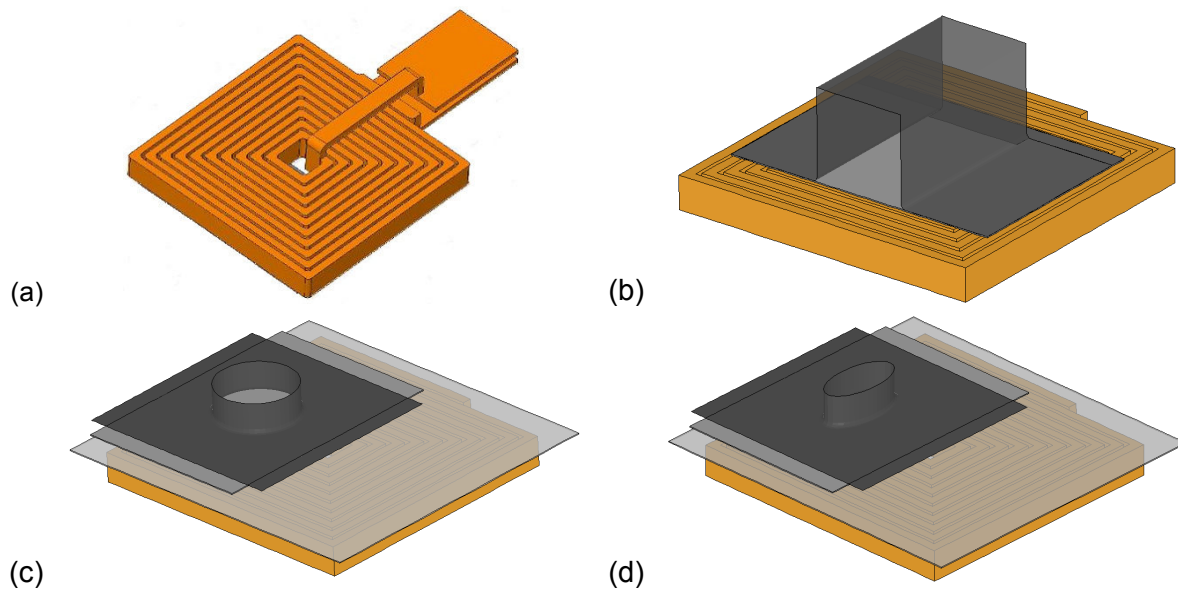
**Figure 5**: *Experimental set-up for the different configurations used. (a) geometry of the coil, (b) square free forming set up, (c) circular and (d) elliptic dies with the driver*
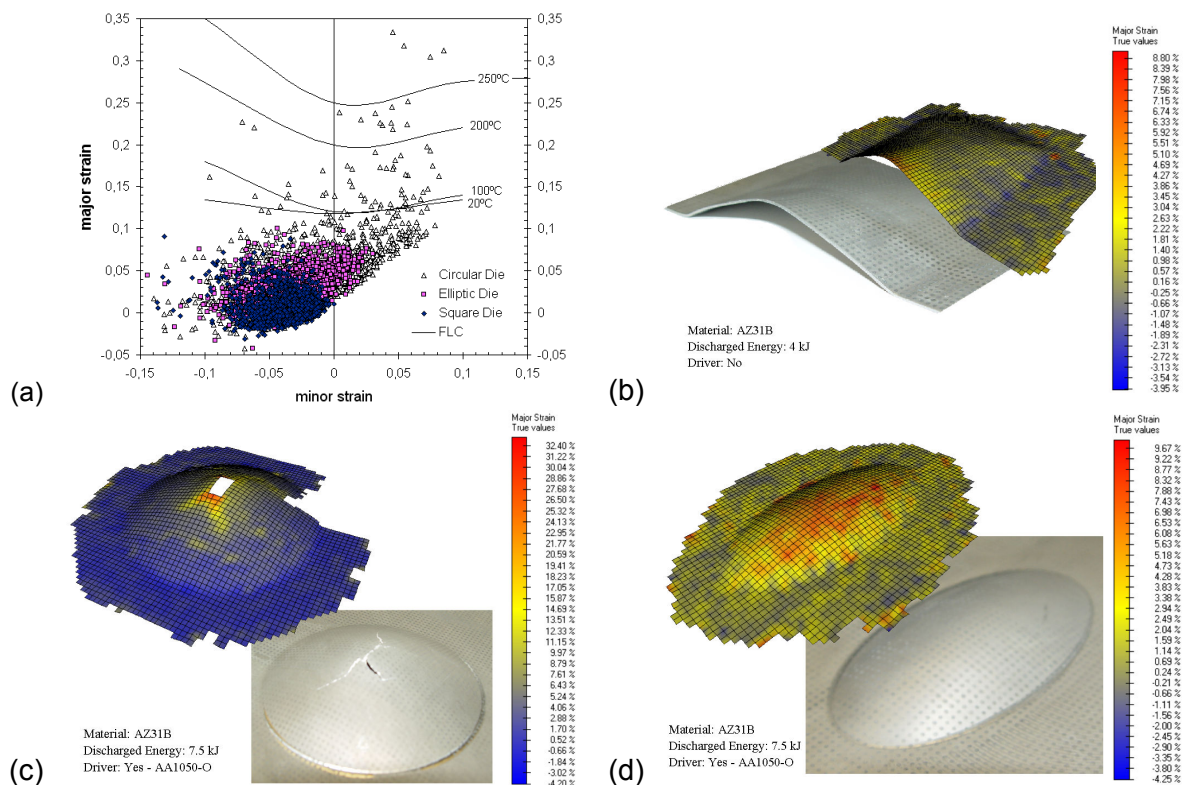


**Figure 6**: *Deformation measurements of the different samples. (a) FLD for the different geometries formed, the FLC curves correspond to [6,14]; formed specimens and measured major strains for (b) square free forming, (c) circular and (d) elliptic dies*

## 3.2   Formability Results of AZ31B Sheet at High Strain Rates

AZ31B sheets were electrochemically etched with a 2 mm x 2 mm square grid before being formed by means of electromagnetic pulses. Once the specimens were formed, the deformation was measured using photogrammetric techniques with the software PHAST® as shown in Figure 6.

The specimens formed using each configuration and the measured major strains are displayed in Figure 6. The different maximum safe deformation states are shown in Figure 6(a) for each die configuration. It can be seen that for circular die forming the maximum deformation values of safe points clearly exceed the conventional Forming Limit Curve (FLC) obtained at room temperature by Palumbo *et al.* [14], showing a positive strain rate sensitivity. The general tendency of increasing the ductility at high strain rates seen for uniaxial tests (Figure 3) is also applicable for biaxial deformations. It is also remarkable that some safe maximum deformation states are close to the FLC curve established by Zhang et al. [6] for warm forming conditions of AZ31B. In the case of the elliptic die forming fracture occurred at the base radius, and so it was impossible to measure higher biaxial deformation values in the top of the geometry. In the case of square of square forming, the material flowed to the deformed part resulting in smaller deformation values.

## 4   Numerical Model

The analysis of EMF process involves the combined study of electromagnetic, mechanical and thermal fields. Consequently numerical simulations of the process must couple these related fields. There are different coupling strategies as explained in [15] and a sequentially coupling method is used in the current work. (Equations of the model are not shown here for briefness and reader is referred to [16] for more information).

Historically, Finite Element Method modelling has been predominantly used for EMF simulations [17], where other methods, such as Smooth Particle Hydrodynamics (e.g. [18]), have not succeeded. In the current study an alternative method is used for computing the electromagnetic fields in the EMF process simulation. A combination of the Finite Element Method (FEM) for conductor parts and the Boundary Element Method (BEM) for the insulators (including air) as implemented in the LS-DYNA commercial code [19], were used to simulate the forming process.

The principal advantage of using the BEM for the air analysis is that it does not need an air mesh. Thus it avoids the meshing problems associated with the air, which can be significant for complicated conductor geometries. EMF simulations include, very small gaps between conductors, leading to a large number of very small and distorted elements which then require re-meshing techniques to be employed as the air mesh moves around the conductors. Another advantage of the BEM is that it does not need the introduction of somewhat artificial infinite boundary condition.

On the other hand, the main disadvantage of the BEM is that it generates full dense matrices in place of the sparse FEM matrices. This causes an *a priori* high memory requirement as well as longer CPU time to solve the linear systems. In order to improve these requirements, a domain decomposition coupled with low rank approximations of the non diagonal sub-blocks of the BEM matrices has been introduced.

The purpose of the numerical study of the current paper is to predict and optimise the final deformed part as well as to outline the influence of different input variables on the final results.

The coil shown in Figure 5(a) was modelled for the EMF process simulation. Firstly the disposition of the workpiece with respect to the coil was studied in order to optimise the discharged energies. Figure 7(a) shows the maximum induced forces for each configuration subjected to an identical input discharged current (Figure 7(b)). It can be seen that when the currents induced in the workpiece form a closed loop, the forces induced in the material are higher. However, the induced currents (i.e. forces) in the sheet location corresponding to the central point of the coil are so small that it does not deform.

Once the suitable configuration was established for each experiment, a comparison between the experimental deformation and the numerical deformation was performed and the results are shown in Figure 8. From the figure, it can be identified that the predicted numerical and experimental temporal shape profiles are in good correspondence. This also indicates that the isotropic material behaviour assumption made in this study (employing constitutive equation explained in section 2) is acceptable, although it is well known the anisotropy on the mechanical behaviour of magnesium alloys at room temperature (e.g. [4]). A possible justification for the difference between experimental and numerical results for the circular die forming experiment (Figure 8(b)) could be the assumption of considering AZ31B sheet as an insulator in the EM analysis, since a driver was used. In the case of temporal study (Figure 8(a)) the reason for the difference could be a result of the excessive material flowing due to incorrect modelling of the friction conditions.

The influence of the conductivity of AZ31B alloy was numerically analysed. The values for conductivity used were those presented in reference [9] where a conductivity range of 9-11 MS/m was measured for AZ31B alloy. In Figure 8(a) it can be seen that the difference between the two conductivities is not very significant.
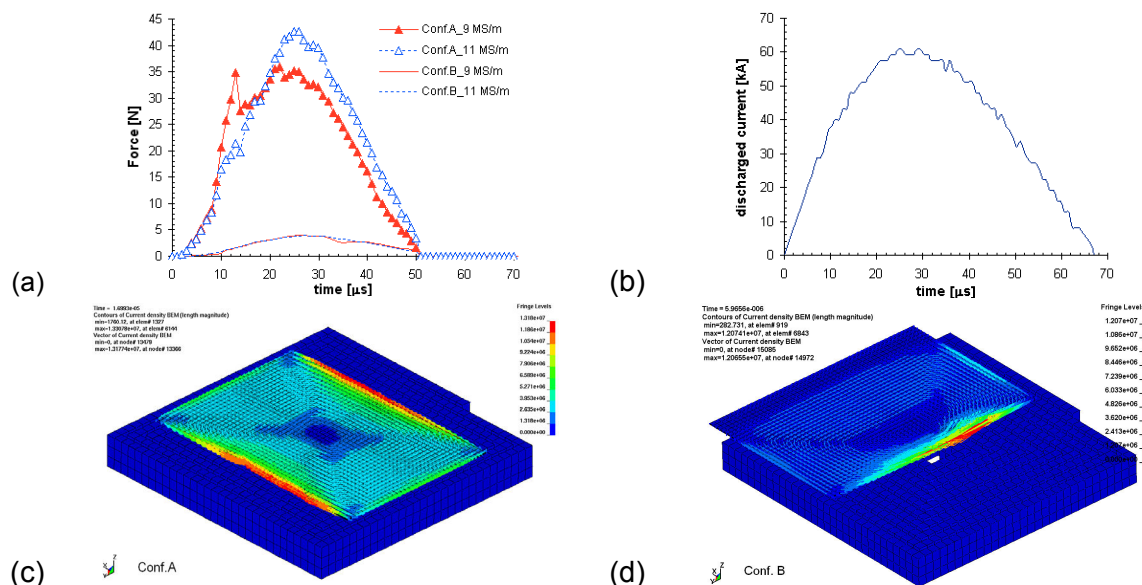


(a) (b) (c) (d)

Figure 7: Numerical results. (a) Influence of the configuration and electrical conductivity of the sample on the induced force; (b) discharged current; vectors of induced current densities (values are in mA/mm$^2$) for (c) Conf.A, (d) Conf.B
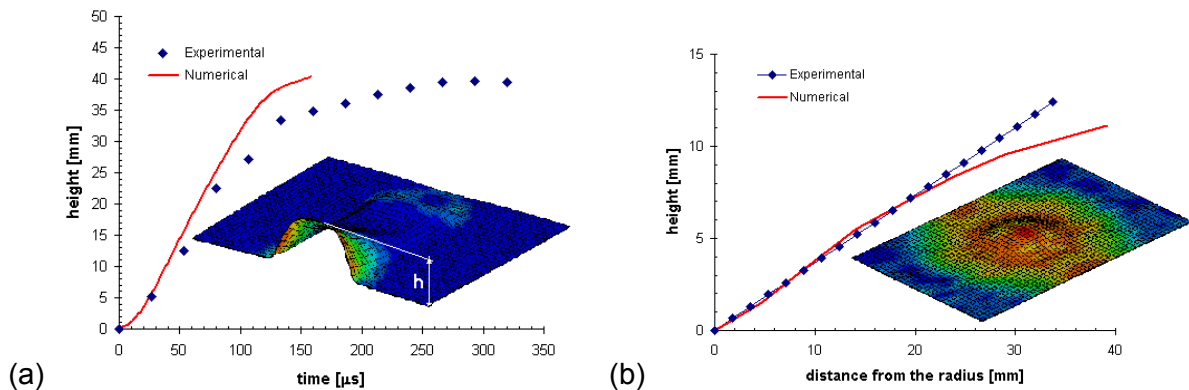
*Figure 8*: Comparison between experimental and numerical results. (a) time evolution of the maximum height for the square forming; (b) final shape for the circular die forming.

## 5 Conclusions

Magnesium alloy AZ31B exhibits significant strain rate sensitivity, with increases in both ductility and flow stress at high strain rates. The estimated parameters for the simplified Johnson-Cook constitutive model fit reasonably well with the experimental data.

Furthermore, biaxial formability tests show that magnesium alloy AZ31B shows improved formability when formed at high strain rates using EMF. It has been suggested that at high strain rates twinning is the most active deformation system [20]. In the future, warm electromagnetic forming will be analysed in order to achieve proper process parameters.

The coupled numerical model suggested in the present contribution allows for the optimization of process parameters, such as sheet-coil configuration and the discharged current values. The numerical results of the deformed parts show relatively good results in comparison with experimental data. In order to obtain more accurate results, a more exhaustive tribological response of the material should be studied. Furthermore, in the case of simulating electromagnetic forming aided with a driver sheet, the AZ31B magnesium sheet should be considered as conductor and induced forces should be computed.

## References

[1]    *Vinarcik, E.J.:* Opportunities of Magnesium Sheet in Automotive Lightening. Light Metal Age, v.55, 1997, p.24-28.

[2]    *Kleiner, M., Geiger, M., Klaus, A.:* Manufacturing of Lightweight Components by Metal Forming. 53rd CIRP General Assembly, Montreal, Canada, 2003, p.521-532.

[3]    Magnesium Vision 2020: A North American Automotive Strategic Vision for Magnesium. USAMP report, 2007.

[4]    *Agnew, S.R., Duygulu, Ö.:* Plastic anisotropy and the role of non-basal slip in magnesium alloy AZ31B. International Journal of Plasticity, v.21,2005, p.1161-1193.

[5]    *Doege, E., Dröder, K.:* Sheet Metal Forming of Magnesium Wrought Alloys – formability and process technology. Journal of Materials Processing Technology, v.115, 2001, p.14-19.

[6] *Zhang, K.F., Yin, D.L., Wu, D.Z.:* Formability of AZ31 magnesium alloy sheets at warm working conditions. International Journal of Machine Tools & Manufacture, v.46, 2006, p.1276-1280.

[7] *El-Magd, E., Abouridouane, M.:* High Speed Forming of the Light-Weight Wrought Alloys, Proceedings of the First International Conference on High Speed Forming, Dortmund, 2004, p.3-12.

[8] *Jimbert, P., Ulacia, I., Fernández, J.I., Eguia, I., Gutierrez, M., Hurtado, I.:* New Forming Limits By Means Of Electromagnetic Forming And Numerical Simulation of The Process. 10th ESAFORM Conference on Material Forming. AIP Conference Proceedings, v.907, 2007, p.1295-1300.

[9] *Psyk, V., Beerwald, C., Klaus, A., Kleiner, M.:* Characterisation of extruded magnesium profiles for electromagnetic joining. Journal of Materials Processing Technology, v.177, 2006, p.266-269.

[10] *Revuelta, A., Larkiola, J., Coronen, A.S., Kanervo, K.:* High Velocity Forming of Magnesium and Titanium Sheets. 10th ESAFORM Conference on Material Forming. AIP Conference Proceedings, v.907, 2007, p.157-162.

[11] *Uhlmann, E., Jurgasch, D.:* New Impulses in the Forming of Magnesium Sheet Metals, Proceedings of the First International Conference on High Speed Forming, Dortmund, 2004, p.229-241.

[12] *Ulacia, I., Salisbury, C.P., Hurtado, I., Worswick, M.J.:* High strain rate characterization of AZ31B magnesium alloy sheet. In preparation. 2008.

[13] *Johnson, G.R., Cook, W.H.:* A constitutive model and data for metals subjected to large strain, high strain rates and high temperature. 7th International Symposium on ballistics, 1983, p.541-547.

[14] *Palumbo, G., Sorgente, D., Tricarico, L., Zhang, S.H., Zheng, W.T., Zhou, L.X.:* Formability Evaluation in Warm Conditions of AZ31 Magnesium Alloy. Proceedings of the IDDRG Conference, Porto, 2006, p.59-66.

[15] *Kleiner, M., Brosius, A., Blum, H., Suttmeier, F.T., Stiemer, M., Svendsen, B., Unger,J., Reese, S.:* Benchmark Simulation for Coupled Electromagnetic-Mechanical Metal Forming Processes. Production Engineering, v.XI, 2004, p.85-90.

[16] *Ulacia, I., Imbert, J., L'Eplattenier, P., Hurtado, I., Worswick, M.J.:* Numerical simulation of electromagnetic forming process using a combination of BEM and FEM. Submitted to Numisheet08, September 1-5, 2008, Interlaken, Switzerland.

[17] *El-Azab, A., Garnich, M., Kapoor, A.:* Modeling of the electromagnetic forming of sheet metals: state-of-the-art and future needs. Journal of Materials Processing Technology, 2003, v.142, p.744-754.

[18] *Panshikar, H.M.:* Computer modeling of electromagnetic forming and impact welding, M.S. Thesis, Ohio State University, 2000.

[19] *L'Eplattenier, P., Cook, G., Ashcraft, C., Burger, M., Shapiro, A., Daehn, G., Seth, M.:* Introduction of an Electromagnetism Module in LS-DYNA for coupled Mechanical-Thermal-Electromagnetic Simulations. Proceedings of the 9th International LS-DYNA Users Conference, Dearborn, 2006, p.17/1-17/8.

[20] *Kintana, J., Ulacia, I., Salisbury, C.P., Hurtado, I., Worswick, M.J.:* Comportamiento de la aleación de magnesio AZ31B a altas velocidades de deformación y elevadas temperaturas. To be published in the proceedings of the X Congreso Nacional de Materiales, June18-20, 2008, Donostia, Spain.